

4-Membered metallodithiophosphinate rings – flat or puckered? A comparison of two crystal structures with computational and literature data

Catharine Esterhuysen ^{a,*}, Gert J. Kruger ^{b,1}, Gavin Blewett ^a, Helgard G. Raubenheimer ^a

^a Department of Chemistry, University of Stellenbosch, Private Bag XI, Stellenbosch, Matieland 7602, South Africa

^b Department of Chemistry and Biochemistry, University of Johannesburg, P.O. Box 524, Auckland Park, 2006, South Africa

Received 13 July 2005; accepted 2 October 2005

Available online 22 November 2005

Abstract

Two crystalline forms of (dithiodiphenylphosphinate)(phenyl)(triphenylphosphine)-palladium(II) ($C_{36}H_{30}P_2PdS_2$), one without solvent, the other containing THF (C_4H_8O), are obtained after reaction of sodium diphenyldithiophosphinate with (phenyl) (bis-triphenylphosphine) palladium(II) chloride and crystallisation from two different solvent mixtures. The molecular structures, as determined by single crystal X-ray diffraction, differ in the planarity of the 4-membered palladium dithiophosphinate rings. The experimental conformations have been compared to the conformations of four-membered metal-S₂P rings reported in the Cambridge Structural Database. A flat conformation is more common than a puckered one. DFT calculations at the B3LYP level of theory indicate that the flat conformation of a model metallodithiophosphinate ring is very slightly lower in energy (1.2 kcal/mol) than the puckered conformation.

© 2005 Elsevier B.V. All rights reserved.

Keywords: X-ray crystal structures; 4-Membered rings; Palladium complexes

1. Introduction

In the course of an ongoing study into improving catalysts for alkene oligomerisation, we have focussed on preparing model palladium complexes of bidentate ligands that could exhibit hemilabile properties [1]. Our interest turned to dithiophosphinate compounds as possible candidates, since they can coordinate to virtually all main group and transition metals in a variety of coordination modes [2], including monodentate (with only one S atom coordinating to the metal) and bidentate modes (where four-membered rings are formed), as indicated in Scheme 1.

Coordination patterns **b** and **c** are characterised formally by a dative bond between the metal and the second

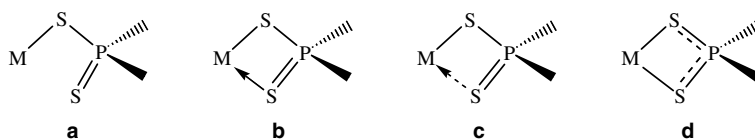
coordinating sulphur, which is slightly (in **b**) or significantly (in **c**) longer than the covalent metal-sulphur bond. The metal-sulphur bond lengths in coordination pattern **d** are approximately the same, as are the P–S separations, due to delocalisation of the negative charge. In both **b** and **c** the P–S double bond is retained, although the double bond character may be slightly affected by the coordination. It has been suggested that the coordination mode is dependent on the metal involved, and the ligand surrounding it; with soft metal centres coordination modes **a–c** are preferred, while harder metals tend to coordinate in mode **d** [2].

This paper describes the preparation and analysis of a diphenyldithiophosphinate complex of palladium, $C_{36}H_{30}P_2PdS_2$ (Scheme 2). NMR analysis gave no indication that the ligand was hemilabile, nevertheless two sets of crystals exhibiting different crystal morphology were obtained when the complex was crystallised from two different solvent mixtures. In order to investigate the possibility that

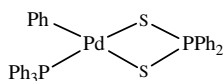
* Corresponding author. Tel.: +27 21 8083345; fax: +27 21 8083360.

E-mail addresses: ce@sun.ac.za (C. Esterhuysen), gjk@na.rau.ac.za (G.J. Kruger).

¹ Tel.: +27 11 4892368; fax: +27 11 4892819.



Scheme 1.



Scheme 2.

the two could contain the ligand in two different coordination modes both were analysed by single crystal X-ray diffraction. The product complex exhibited two different conformations: in the crystal without solvent (hereafter designated **1**), the 4-membered metallo-dithiophosphinate ring was shown to be distorted from planarity, as opposed to planar in the crystal that contained THF (hereafter designated **2**). To better understand the reasons for such different behaviour, and also establish the occurrence of energy differences between such conformations we undertook an analysis of similar compounds in the Cambridge Structural Database (CSD) [3] and compared the two conformations in an *ab initio* computational study.

2. Experimental

2.1. General procedures and instruments

All reactions and manipulations were carried out under a dry argon atmosphere using standard Schlenk and vacuum-line techniques. All solvents were dried and purified by conventional methods and were freshly distilled under argon shortly before use. Other reagents were used without further purification. NMR spectra were measured on a Varian VXR 300 spectrometer (^1H , 300 MHz; ^{13}C , 75.48 MHz; ^{31}P , 127.4 MHz) at 20 °C. Chemical shifts are reported in ppm relative to signals for residual ^1H and ^{13}C atoms in the deuterated solvents.

2.2. Synthesis

Diphenyldithiophosphinic acid, 0.121 g (4.84×10^{-4} mol), was dissolved in 1 ml of methanol and 2 ml of THF. 2.42×10^{-4} mol dry sodium carbonate (0.026 g) was added and the mixture stirred for 1 h. The solution was then evaporated to dryness to deliver a colourless product that was placed under high vacuum for extended periods to ensure all the water formed was removed. 0.073 g (2.69×10^{-4} mol) of this sodium salt was dissolved in 7 ml of anhydrous THF and added dropwise to 0.200 g (2.69×10^{-4} mol) $(\text{PPh}_3)_2\text{Pd}(\text{Ph})(\text{Cl})$ [4] and stirred vigorously for 36 h. The reaction mixture turned yellow during this period. The solution was filtered through an anhydrous

celite-packed sintered glass filter and evaporated to dryness. The product was purified by crystallisation from mixed solvents. The 1:1 mixtures of THF/pentane and benzene/pentane, respectively, yielded the distinctly different solvated and non-solvated batches of crystals.

Complex $\text{C}_{36}\text{H}_{30}\text{P}_2\text{PdS}_2$: colourless crystalline material, yield: 0.112 g, 58%. ^1H NMR (300 MHz, CDCl_3 , 20 °C): $\delta = 7.83\text{--}7.91$ (m, 4H), 7.21–7.44 (m, 21H, PPh_3 , $(\text{Ph})_2\text{PS}_2\text{H}$), 7.01–7.05 (m, 2H, C_6H_5), 6.66–6.68 (m, 3H); $^{13}\text{C}\{^1\text{H}\}$ NMR (75 MHz, CDCl_3 , 20 °C): $\delta = 136.0$ (d, $J_{\text{C-P}} = 4.1$ Hz, 1H), 134.4 (d, $J_{\text{C-P}} = 11.7$ Hz), 131.2 (d, $J_{\text{C-P}} = 3.1$ Hz), 131.0 (s), 130.6 (s), 130.4 (s), 130.2 (d, $J_{\text{C-P}} = 2.4$ Hz), 130.0 (d, $J_{\text{C-P}} = 11.7$ Hz), 128.3 (d, $J_{\text{C-P}} = 13.1$ Hz), 128.2 (d, $J_{\text{C-P}} = 10.3$ Hz), 128.1 (d, $J_{\text{C-P}} = 7.9$ Hz), 127.4 (s), 122.7 (s); $^{31}\text{P}\{^1\text{H}\}$ NMR (121 MHz, CDCl_3 , 20 °C): 77.29 (d, 1P) ($J = 7.3$ Hz), 30.12 (d, 1P) ($J = 6.8$ Hz).

2.3. X-ray structure determination

Colourless crystals suitable for X-ray structure determination were obtained by crystallisation from a solution of dichloromethane layered in a 1:1 ratio with pentane (**1**). Crystallisation from a solution of tetrahydrofuran (THF) layered in a 1:1 ratio with pentane yielded orange crystals containing included solvent (**2**). Data were collected on a Siemens SMART diffractometer [5] at room temperature with graphite monochromated Mo $\text{K}\alpha$ radiation and corrected for Lorentz and polarization effects [6]. Empirical absorption corrections were applied [7]. The structures were solved by interpretation of a Patterson synthesis which yielded the positions of the metal atoms. All non-hydrogen atoms were refined anisotropically by full-matrix least-squares calculations on F^2 using SHELXL-97 [8] within the X-seed environment [9]. The presence of extra peaks of electron density on the difference Fourier map indicated the existence of disorder in the dithiophosphinate complex in **2**, with second atomic positions being located for the Pd, both S atoms and P(2). The positions of these four atoms could be refined, with anisotropic displacement parameters for the Pd, while the site occupancy refined to 5%. This small contribution by the minor component meant that the positions of the carbon atoms could not be identified from the difference Fourier map, and thus the remainder of the disordered portion was not further modelled. Further details of the data collections and structure refinements are listed in Table 1. ORTEP-3 for Windows [10] was used to generate the figures, with ellipsoid probabilities at 50%.

Table 1
Crystal data and structure refinement for complexes **1** and **2**

	1	2
Empirical formula	C ₃₆ H ₃₀ P ₂ PdS ₂	C ₃₆ H ₃₀ P ₂ PdS ₂ · C ₄ H ₈ O
Formula weight (g mol ⁻¹)	695.06	767.16
Temperature (K)	296(2)	296(2)
Crystal system, space group	monoclinic, P2 ₁ /n	triclinic, P $\bar{1}$
<i>Unit cell dimensions</i>		
<i>a</i> (Å)	12.9199 (6)	10.9884 (6)
<i>b</i> (Å)	16.2919 (8)	3.2742 (7)
<i>c</i> (Å)	15.9092 (8)	13.4552 (7)
α (°)	90	88.534 (1)
β (°)	103.777 (1)	83.825 (1)
γ (°)	90	71.356 (1)
<i>V</i> (Å ³)	3252.4 (3)	1848.74 (17)
<i>Z</i>	4	2
Calculated density (Mg m ⁻³)	1.419	1.378
Absorption coefficient (μ) (mm ⁻¹)	0.821	0.731
<i>F</i> (000)	1416	788
Crystal size	0.38 × 0.32 × 0.25	0.35 × 0.35 × 0.25
θ Range for data collection (°)	1.82–25.00	1.52–25.00
Index ranges	-15 ≤ <i>h</i> ≤ 13, -19 ≤ <i>k</i> ≤ 19, -15 ≤ <i>l</i> ≤ 18	-13 ≤ <i>h</i> ≤ 13, -15 ≤ <i>k</i> ≤ 15, -15 ≤ <i>l</i> ≤ 12
Reflections collected/unique [<i>R</i> _{int}]	16 679/5661 [0.0437]	9840/6230 [0.0489]
Completeness to maximum 2 θ	98.9%	95.9%
Refinement method	full-matrix least-squares on <i>F</i> ²	full-matrix least-squares on <i>F</i> ²
Data/restraints/parameters	5661/0/370	6230/2/458
Goodness-of-fit on <i>F</i> ²	1.087	1.201
Final <i>R</i> indices [<i>I</i> > 2 σ (<i>I</i>)]	<i>R</i> ₁ = 0.0466, <i>wR</i> ₂ = 0.0715	<i>R</i> ₁ = 0.0577, <i>wR</i> ₂ = 0.1210
<i>R</i> indices (all data)	<i>R</i> ₁ = 0.0733, <i>wR</i> ₂ = 0.0785	<i>R</i> ₁ = 0.0698, <i>wR</i> ₂ = 0.1287
Largest difference in peak and hole (e Å ⁻³)	0.426 and -0.329	0.910 and -0.506

2.4. CSD analysis and computational details

The February 2005 version of the CSD (338445 entries) was searched using ConQuest [11] for all structures containing a 4-membered metal-dithiophosphinate ring, M–S–P–S with M = any metal. The data were analysed using Vista, as part of the CSD suite of programs [3].

All calculations were performed using GAUSSIAN-98 [15] at the non-local DFT level of theory with Becke's 3-parameter exchange functional [12] mixed with Lee–Yang–Parr's correlation functional (B3LYP) [13], using the LANL2DZ basis set [14]. Simplified model complexes were used, where the phenyl rings in the structures obtained from the X-ray diffraction analyses were replaced by methyl groups. Geometry optimisations of both conformations were performed, with vibrational frequency calculations used to confirm that minimum energy conformations had been obtained.

3. Results and discussion

3.1. Molecular structures from single-crystal X-ray diffraction analysis

The molecular structure and numbering scheme of **1** are shown in Fig. 1. Selected bond lengths and angles are listed in Table 2. As can be seen from Table 2, the conformation of the minor disorder component is poorly defined, hence most of the discussion will focus on the 95% disordered structure. The ligands are arranged around the Pd in a

square-planar configuration, with the dithiophosphinate ligand coordinating bidentately to form a 4-membered Pd–S–P–S metallocyclic ring. The overall molecular structure of **2** is similar, although there are significant differences in the central core, including the conformation of the 4-membered Pd–S–P–S ring. In order to more clearly appreciate the differences Fig. 2 shows the spheres of coordination around the Pd atoms.

In **1** the deviation from the square-planar configuration around the Pd is more pronounced than in **2**, with a maximum deviation from planarity of 0.135 (1) Å by C(31) in **1**, compared to 0.038(2) Å by C(31) in **2**. The two Pd–S separations are significantly different in both **1** and **2**, with the effect being more pronounced in **2**, where the difference between Pd–S(1) and Pd–S(2) is 0.11 Å for the major disorder component (although only 0.01 Å for the minor component), suggesting that the dithiophosphinate ligand is coordinating according to either pattern **b** or **c** in Scheme 1. However, at the same time the difference in S–P bond lengths in each compound is negligible, thus implying that coordination mode **d** should also be considered in both complexes, despite Pd²⁺ being a soft metal. The longer Pd–S(2) distance can instead be attributed to the larger *trans* influence of the phenyl group compared to the phosphine.

In **1** the ring is strongly puckered, as seen in Fig. 2(a), with P(1) lying 1.188(1) Å above the plane containing Pd, S(1) and S(2) and the puckering angle between the Pd–S(1)–S(2) and P(1)–S(1)–S(2) planes being 23.2(1)°, whereas the ring in **2** (Fig. 2(b) and (c) – major and minor

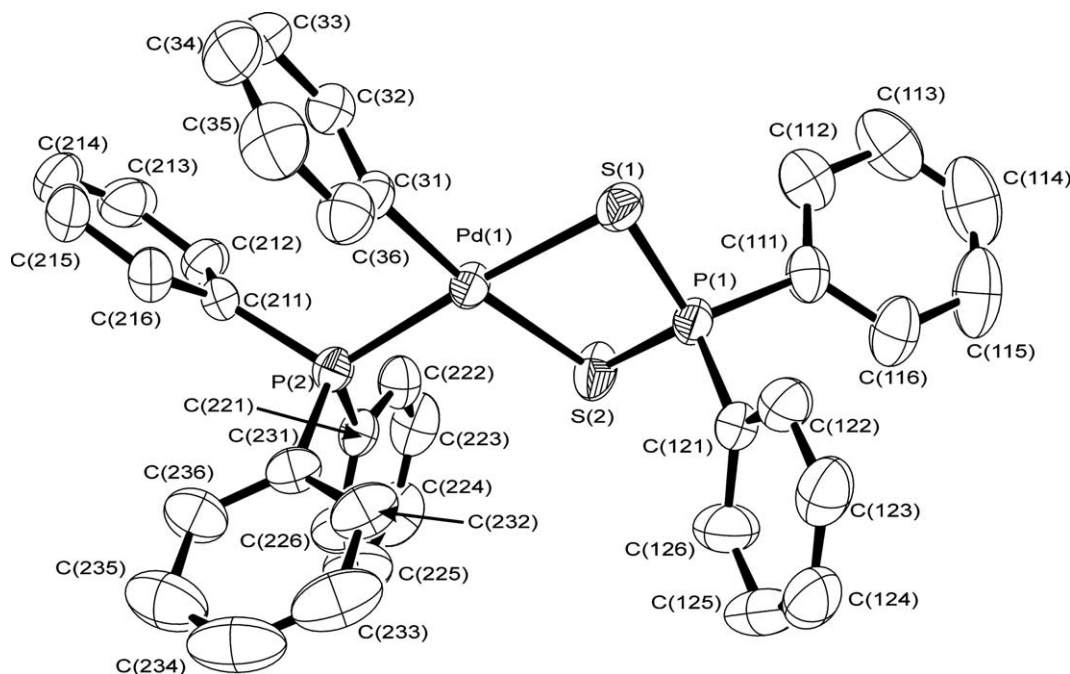


Fig. 1. Molecular structure and numbering scheme of **1**. Hydrogens are omitted for clarity. Ellipsoids are shown at the 50% probability level.

Table 2

Selected bond distances (Å) and angles (°) for **1** and **2**

	1	2 ^a	Pd–S–P–S ^b	M–S–P–S ^c
<i>Bond distances</i>				
Pd–C(31)	2.007(4)	2.015(6)		
Pd–P(2)	2.2534(10)	2.2628(14)		
		[2.23(3)]		
Pd–S(1) ^d	2.4029(10)	2.3845(17)	2.35(3)	2.51(13)
		[2.38(4)]		
Pd–S(2)	2.4571(11)	2.493(2)	2.37(3)	2.57(18)
		[2.39(4)]		
S(1)–P(1)	2.0142(14)	2.008(2)	2.01(2) ^e	1.99(3) ^e
		[1.99(2)]		
S(2)–P(1)	2.0108(14)	2.005(2)		
		[2.04(2)]		
Pd–P(1)	2.956(1)	2.990(1)	2.99(6)	3.14(14)
		[3.04(1)]		
<i>Bond angles</i>				
S(1)–Pd–S(2)	83.33(3)	83.68(6)	83.5(9)	78(4)
		[82.2(7)]		
Pd–S(1)–P(1)	83.52(4)	85.32(7)		
		[87.5(11)]		
Pd–S(2)–P(1)	82.20(5)	82.56(8)		
		[86.3(12)]		
S(1)–P(1)–S(2)	106.78(6)	108.36(9)	103(3)	107(3)
		[102.1(16)]		

Average literature values calculated from CSD data are included for comparison.

^a Values for minor disorder component given in parenthesis.

^b Average value calculated from 25 fragments in 19 structures, standard deviation in parenthesis.

^c Average value calculated from 1006 fragments in 499 structures, standard deviation in parenthesis.

^d Pd–S bond lengths were chosen so that Pd–S(1) < Pd–S(2).

^e Average for S(1)–P(1) and S(2)–P(1).

disorder components, respectively), is planar, with P(1) bent only 0.065(3) Å away from the Pd–S(1)–S(2) plane (at puckering angles of 3.0(1)° and 7(1)° for the major and minor disorder components, respectively). The puckering can also be measured by the Pd–S(1)–P(1)–S(2) torsion angle, which is 17.45(6)° in the distorted ring in **1**, as

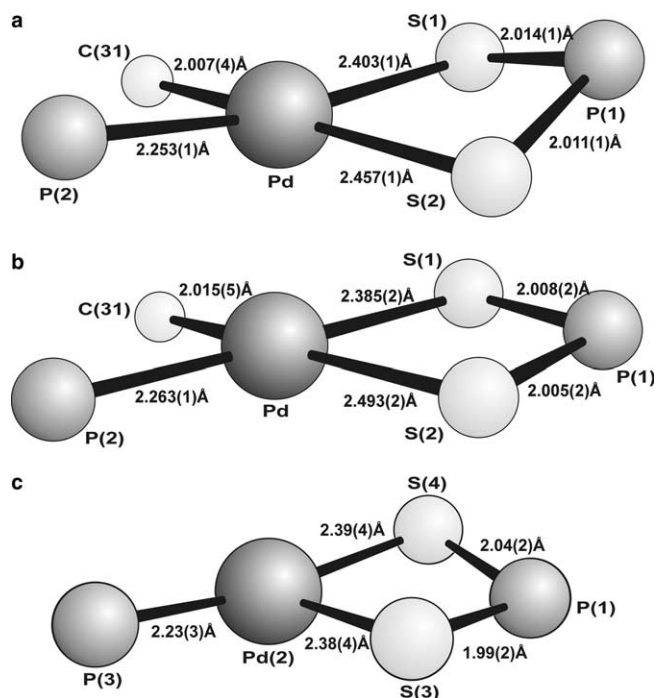


Fig. 2. Sphere of coordination around Pd for (a) **1**, (b) major disorder component of **2** and (c) minor disorder component of **2**.

opposed to only $2.31(10)^\circ$ in **2** ($11.4(14)$ for the minor disorder component). The puckering observed means that in **1** the Pd to P(1) distance is shorter than in **2** ($2.956(1)$ Å as opposed to $2.990(2)$ Å or $3.04(1)$).

This puckering in the solid state can be ascribed to the C(12X) phenyl ring on the diphenyldithiophosphinate ligand being involved with five different weak off-set face-to-edge π – π interactions (see Fig. 3); three to each of the phenyl rings in the triphenylphosphine ligand on a neighbouring molecule (coloured purple), one to a triphenylphosphine group on a second neighbouring molecule (coloured red) and the fifth to the phenyl ligand on a third neighbouring molecule (coloured blue) with face-to-edge separations of 2.87, 2.99, 3.08, 2.97 and 2.98 Å, respectively (see Table 3). The P···P distance to the purple coloured molecule is $7.116(1)$ Å. These distances agree well with values given for so-called “phenyl embraces” by Dance and Scudder [16], who suggest C···H distances of 2.8–3.2 Å, and P···P distances of 6.4–7.4 Å. In order to maximise these interactions the diphenyldithiophosphinate ligand needs to bend away from the molecular plane as observed. A further off-set face-to-edge interaction is observed for the second phenyl in the diphenyldithiophosphinate ligand. A smaller number of similar, although weaker, off-set face-to-edge π – π interactions (Table 3) are observed in the crystal structure of **2**, resulting in an extended 3-dimensional network of interlocked molecules with the THF solvent molecules located in narrow channels, as shown in Fig. 4. The P···P distances are longer, $8.244(2)$ Å and $8.611(2)$ Å

Table 3
 π – π interaction distances for **1** and **2** (Å)

1		2	
C(123)···H(236)	2.87	C(124)···H(222)	2.87
C(124)···H(224)	2.97	H(124)···C(213)	3.06
H(126)···C(33)	2.98	C(126)···H(214)	3.08
H(123)···C(226)	2.99	C(122)···H(113)	3.10
H(122)···C(214)	3.08	H(232)···C(213)	2.87
H(213)···C(115)	3.13		

to the purple and blue coloured molecules, respectively. The packing of the molecules relative to each other allows the formation of these intermolecular interactions without the concomitant distortion observed for **1**. Furthermore, the longer separations in **2** suggest that the interactions are weaker and do not supply as much stabilisation to the structure.

3.2. Conformational analysis using CSD

The search for 4-membered $\overline{\text{M-S-P-S}}$ rings (M = any metal) yielded 537 structures, with a total of 1074 fragments, that matched the search criteria. 19 of these contained a $\overline{\text{Pd-S-P-S}}$ ring, with a total of 25 fragments matching the search criteria. The average bond lengths and angles in the $\overline{\text{M-S-P-S}}$ and $\overline{\text{Pd-P-S-P}}$ rings as calculated from these results are listed in Table 4. These values agree well with those in **1** and **2**, except for the average Pd–S bond length, which is shorter than all four Pd–S bond

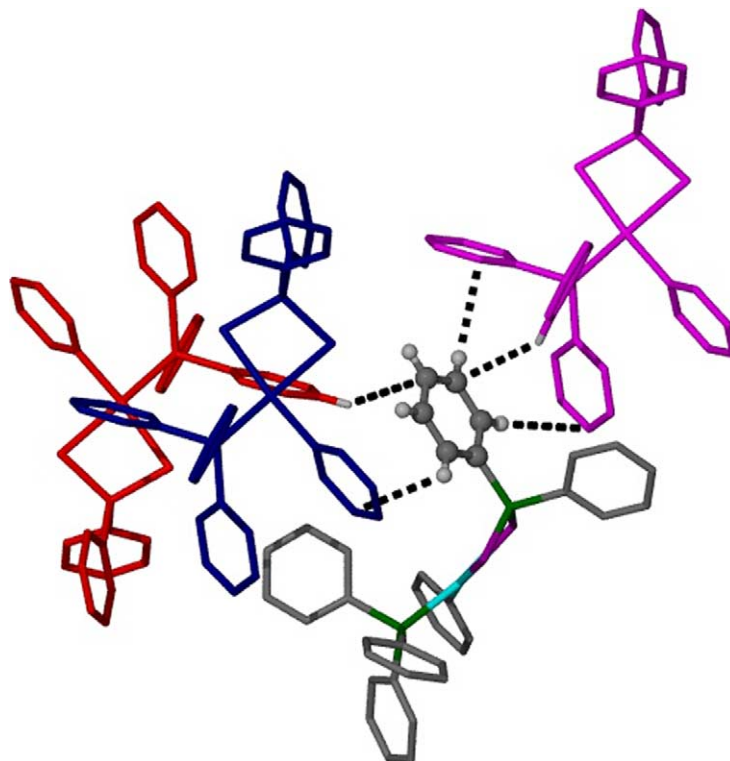


Fig. 3. Off-set face-to-edge π – π interactions formed by the C(12X) phenyl ring in **1**. The three neighbouring molecules are coloured in purple, red and blue, respectively. (For interpretation of the references to colour in this figure legend, the reader is referred to the web version of this article.)

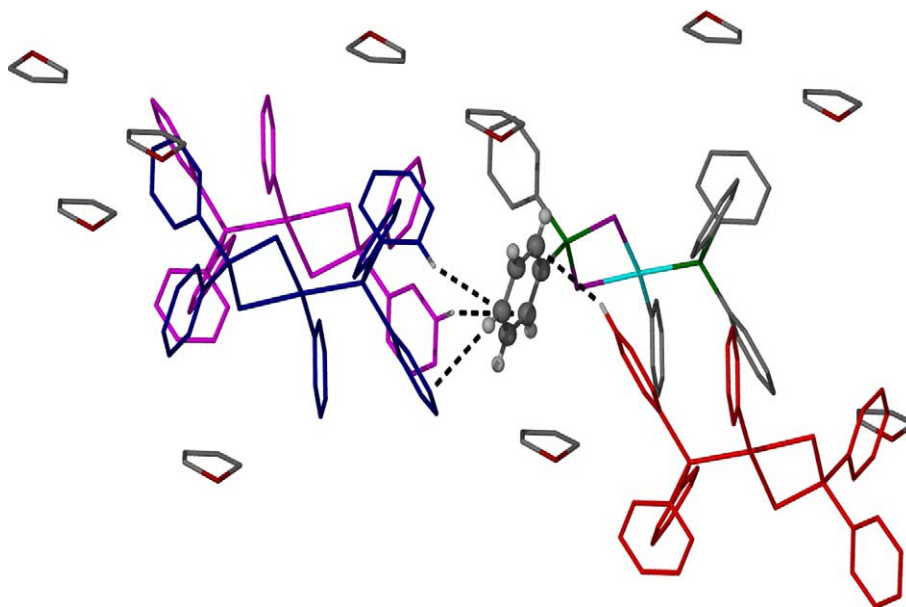


Fig. 4. Off-set face-to-edge π - π interactions formed by the C(12X) phenyl ring in **2**. The three neighbouring molecules are coloured in purple, red and blue, respectively. (For interpretation of the references to colour in this figure legend, the reader is referred to the web version of this article.)

Table 4
Average bond lengths (Å) and angles (°) calculated from the literature structures reported in the CSD

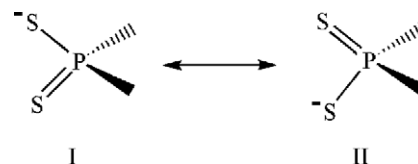
	Parameters in Pd-S-P-S ^a	Parameters in M-S-P-S ^b
Pd-S(1) ^c	2.35(3)	2.51(13)
Pd-S(2)	2.37(3)	2.57(18)
S-P	2.02(3)	1.99(3)
Pd-P	3.00(7)	3.14(14)
S-P-S	103(3)	107(4)
S-M-S	83.5(9)	79(4)

^a Average value calculated from 25 fragments in 19 structures, standard deviation in parenthesis.

^b Average value calculated from 1074 fragments in 537 structures, standard deviation in parenthesis.

^c Pd-S bond lengths were chosen so that Pd-S(1) < Pd-S(2).

lengths in **1** and **2**. In fact, the two Pd-S(2) bond lengths in **1** and **2** are the longest Pd-S bond lengths yet observed in this type of complex. The previous longest Pd-S bond was 2.430 Å [17]. In addition, most of the complexes reported in the literature do not show such a large difference in their two metal-S bond lengths as observed in **2**. In particular, most Pd complexes have coordination mode **d** (Scheme 1), with small differences between P-S and Pd-S bond lengths (the largest differences between Pd-S bond lengths is 0.083 Å) [18]. Only 11.8% of all fragments have a difference in metal-S bond lengths of greater than 0.11 Å. The majority of these are complexes of dithiophosphate ligands with main group metals (In, Tl, Ge, Sn, Pb, Sb, Bi, Te) corresponding with coordination in mode **c** (Scheme 1). Of the transition metal complexes, only 6.3% have metal-S bond lengths that differ by more than the 0.11 Å observed for **2**. In all of these complexes the difference in P-S bond lengths is relatively small, with 93.7% of structures having a difference in P-S bond lengths



Scheme 3.

of less than 0.05 Å, indicating delocalisation in the PS_2^- fragment and suggesting coordination mode **d**.

The two P-S distances can be expected to not differ significantly since there are two resonance structures (Scheme 3). This was confirmed by a search for dithiophosphate anions, which revealed that 91.5% of the 71 structures found had a difference in P-S bond lengths of less than 0.05 Å, just as found in the complexes. The larger differences observed can be explained by packing effects.

The S-M-S-P torsion angle, used as an indicator of the puckering in the S-M-S-P ring, varies between 0° and 22.15° (absolute values of all torsion angles were taken). In order to make a comparison between complexes that can be designated as having a flat conformation and those having a puckered conformation an arbitrary cutoff value of 10° was chosen as indicating a flat geometry. On the basis of this designation 88.9% of all S-M-S-P fragments can be considered flat. These results suggest that the puckered conformation exhibited by **1** is probably the strained conformation, since the flat conformation observed in **2** is more common. In order to test this ab initio calculations were performed.

3.3. Computational results

The two experimentally obtained molecular structures were used as a basis for geometry optimisations, although

with the phenyl rings replaced with methyl groups (in the case of **2** the solvent was omitted in order to directly compare bonding energies). In both cases the geometry optimisation yielded the same minimum energy structure (designated **3**), with a planar conformation of the PdS₂P 4-membered ring. The bond lengths and angles of this minimum energy structure are listed in Table 5, and the sphere of coordination around the Pd is shown in Fig. 5(a). In order to determine the difference in energy between a complex with the ligand in this conformation and one with a puckered conformation a geometry optimisation was performed where the S(2)–Pd–S(1)–P torsion angle was constrained to 17.5°, as in the crystal structure of **1**. The minimum energy conformation thus obtained is designated **4**, and details of the structure are included in Table 5 and

Table 5
Bond lengths (Å) and angles (°) of the optimised model compound, **3**, the optimised model compound with torsion angle S–P–S–Pd fixed at 17.5°, **4**, and the monodentate model compound, **5**

	3	4	5
Pd–S(1)	2.510	2.510	2.448
Pd–S(2)	2.621	2.627	4.283
S(1)–P	2.189	2.189	2.242
S(2)–P	2.181	2.183	2.141
Pd–P	3.212	3.143	3.705
S(1)–P–S(2)	105.4	104.3	118.6
S(1)–Pd–S(2)	85.2	84.4	61.1
S(2)–Pd–S(1)–P	0.0	17.5	26.5

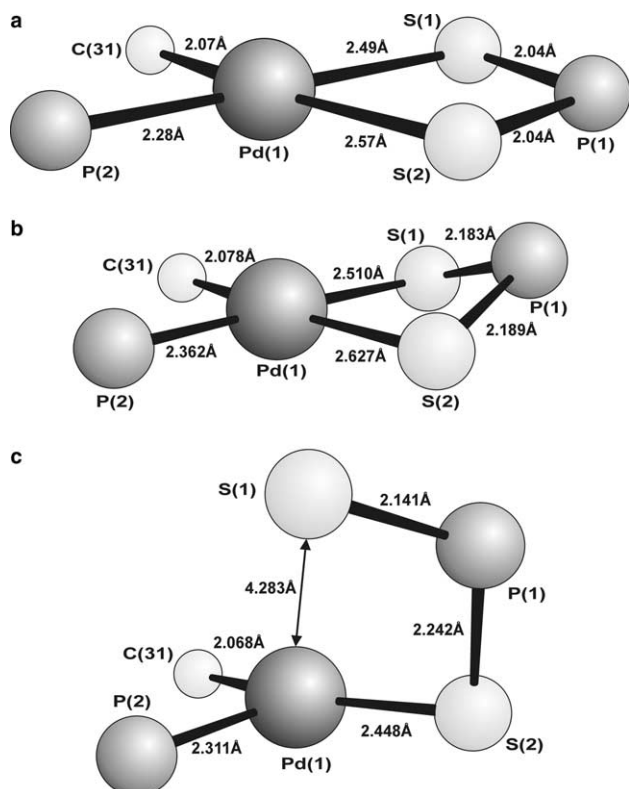


Fig. 5. Sphere of coordination around Pd for (a) **3**, (b) **4**, (c) **5**.

Table 6

Comparison of calculated absolute energies (a.u.) and energy differences (kcal/mol) for the optimised model compound, **3**, the optimised model compound with torsion angle S–P–S–Pd fixed at 17.5°, **4**, and the monodentate model compound, **5**

	Energies (a.u.)	ΔE (kcal/mol)
3	–399.477	
4	–399.474	1.191 ^a
5	–399.448	17.695 ^b

^a $\Delta E = E(\mathbf{4}) - E(\mathbf{3})$.

^b $\Delta E = E(\mathbf{5}) - E(\mathbf{3})$.

Fig. 5(b). A further optimisation was performed to determine whether the dithiophosphinate ligand could coordinate in a monodentate fashion. The corresponding minimum energy conformation is designated **5**, and structural details are also included in Table 5 and Fig. 5(c).

The absolute energies of these three conformations are given in Table 6, along with the difference in energies as compared to the lowest energy conformation, **3**.

The results show clearly that the calculated difference in energy between the flat and puckered conformations is very small, with the flat conformation being more stable than the puckered conformation. The complex with the model ligand in the monodentate coordination mode is much higher in energy, explaining why it is not found experimentally.

The calculated bond lengths are longer than those observed experimentally. However, the trends are similar, with the Pd–S bond lengths differing by 0.11 Å, while the S–P bonds are the same length. The bond lengths in the calculated flat, **3**, and puckered, **4**, conformations do not differ from each other, such as was observed experimentally. Bond angles agree well with experimentally observed values. The short S(1)–P bond length in the monodentately coordinated dithiophosphinate ligand in **5** clearly indicates that it is a double bond, as expected according to Scheme 1a, whereas the S(2)–P bond length indicates a single bond.

4. Conclusion

The results of the CSD analysis and ab initio calculations show that 4-membered PdS₂P rings will take up a flat conformation in the absence of other influencing factors. In the case of the two crystalline forms described crystallographically in this paper, the PdS₂P ring in **1** is distorted from planarity by the dithiophosphinate ligand bending to enable the formation of weak intermolecular π – π interactions between one of the phenyl rings and phenyl rings on neighbouring molecules, whereas for **2** intermolecular π – π interactions can form without distortion and the PdS₂P ring is thus flat.

Acknowledgements

We thank the NRF, the University of Stellenbosch and the University of Johannesburg for funding.

Appendix A. Supplementary material

Crystallographic data for the structural analysis have been deposited with the Cambridge Crystallographic Data Centre, CCDC Nos. 278302 (1) and 278303 (2). Copies of this information may be obtained free of charge from the Director, CCDC, 12 Union Road, Cambridge, CB2 1E2, UK (fax: +44 1223 336 033; e-mail: deposit@ccdc.cam.ac.uk, www: <http://www.ccdc.cam.ac.uk>). Supplementary data associated with this article can be found, in the online version, at doi:10.1016/j.ica.2005.10.006.

References

- [1] M.W. Esterhuysen, H.G. Raubenheimer, R. Brüll, C. Esterhuysen, G.J. Kruger, *J. Organomet. Chem.* 619 (2001) 164.
- [2] (a) I. Haiduc, D.B. Sowerby, S.-F. Lu, *Polyhedron* 14 (1995) 3389; (b) I. Haiduc, D.B. Sowerby, *Polyhedron* 15 (1996) 2469.
- [3] F.H. Allen, *Acta Cryst. B* 58 (2002) 380.
- [4] W.A. Herrmann, C. Broßner, T. Priermeier, K. Öfele, *J. Organomet. Chem.* 481 (1994) 97.
- [5] SMART Data Collection Software, Siemens Analytical X-Ray Instruments Inc., Madison, WI, USA, 1996.
- [6] SAINT Data Reduction Software, Siemens Analytical X-Ray Instruments Inc., Madison, WI, USA, 1996.
- [7] G.M. Sheldrick, SADABS, Siemens Analytical X-Ray Instruments Inc., Madison, WI, USA, 1996.
- [8] G.M. Sheldrick, SHELX-97. Program for Crystal Structure Analysis, University of Göttingen, Germany, 1997.
- [9] L.J. Barbour, *J. Supramol. Chem.* 1 (2001) 189.
- [10] L.J. Farrugia, *J. Appl. Cryst.* 30 (1997) 565.
- [11] I.J. Bruno, J.C. Cole, P.R. Edgington, M. Kessler, C.F. Macrae, P. McCabe, J. Pearson, R. Taylor, *Acta Cryst. B* 58 (2002) 389.
- [12] A.D. Becke, *J. Chem. Phys.* 98 (1993) 5648.
- [13] C. Lee, W. Yang, R.G. Parr, *Phys. Rev. B* 37 (1988) 785.
- [14] (a) P.J. Hay, W.R. Wadt, *J. Chem. Phys.* 82 (1985) 270; (b) W.R. Wadt, P.J. Hay, *J. Chem. Phys.* 82 (1985) 284; (c) P.J. Hay, W.R. Wadt, *J. Chem. Phys.* 82 (1985) 299.
- [15] M.J. Frisch et al., GAUSSIAN 98 (Revision A.7), Gaussian, Inc., Pittsburgh, PA, 1998.
- [16] I. Dance, M. Scudder, *J. Chem. Soc., Chem. Commun.* (1995) 1039.
- [17] J.P. Fackler Jr., L.D. Thompson, I.J.B. Lin, T.A. Stephenson, R.O. Gould, J.M.C. Alison, A.J.F. Fraser, *Inorg. Chem.* 21 (1982) 2397.
- [18] K. Panneerselvam, T.-H. Lu, S.-F. Tung, S. Narayan, V.K. Jain, *Acta Cryst. C* 55 (1999) 541.